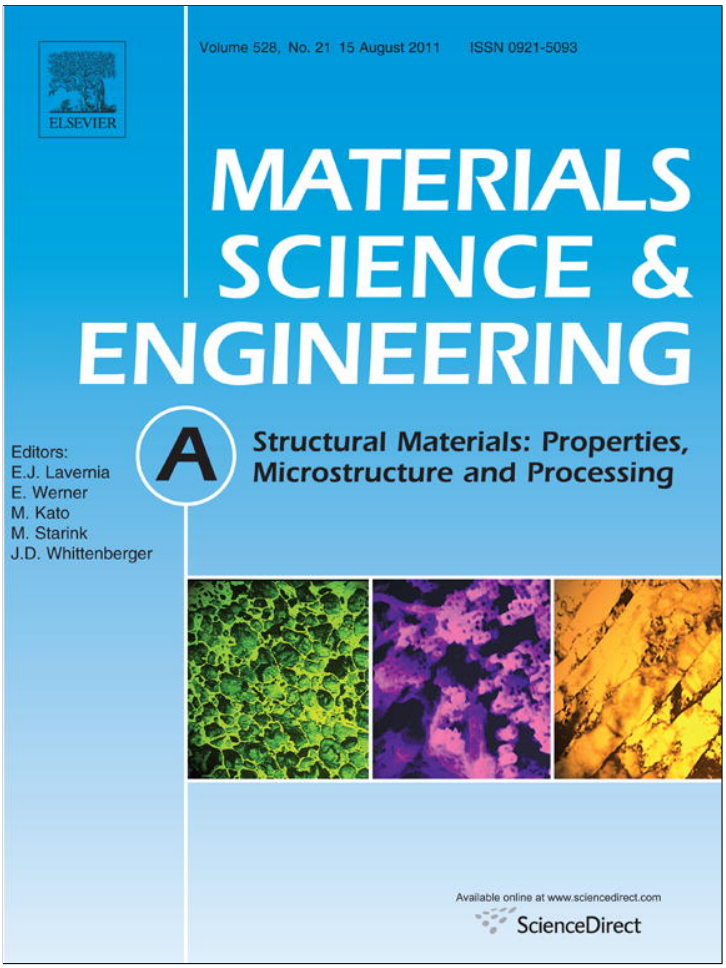

Materials Science and Engineering A 528 (2011) 6636–6641

Contents lists available at ScienceDirect

Materials Science and Engineering A

journal homepage: www.elsevier.com/locate/msea

Mechanical properties of multilayered chitosan/CNT nanocomposite films

Fangfang Sun[a,1], Hee-Ryoung Cha[a,1], KiEun Bae[b], Suckwon Hong[a,b], Jong-Man Kim[a,c], Soo Hyung Kim[a,c], Jaebeom Lee[a,d,*], Dongyun Lee[a,e,*]

[a] Department of Nanofusion Technology, College of Nanoscience and Nanotechnology, Pusan National University, Busan 609-735, Republic of Korea
[b] Department of Nanomaterials Engineering, College of Nanoscience and Nanotechnology, Pusan National University, Busan 609-735, Republic of Korea
[c] Department of Nanomechatronics Engineering, College of Nanoscience and Nanotechnology, Pusan National University, Busan 609-735, Republic of Korea
[d] Department Nanomedical Engineering, College of Nanoscience and Nanotechnology, Pusan National University, Busan 609-735, Republic of Korea
[e] Department of Nanofusion Engineering, College of Nanoscience and Nanotechnology, Pusan National University, Busan 609-735, Republic of Korea

ARTICLE INFO

Article history:
Received 7 April 2011
Accepted 18 May 2011
Available online 26 May 2011

Keywords:
Layered structures
Nanocomposites
Mechanical properties
Interfacial strength
Biopolymer

ABSTRACT

A multi-performance MWCNT-reinforced chitosan nanocomposite was fabricated by two methods: a freeze-drying process associated with the sublimation and compression (SAC) method; and the casting-evaporation (CE) method. We obtained ordered and multilayered structures with limited porosity, and well-dispersed MWCNT structures of the chitosan nanocomposite, especially with the SAC method. In the case of the nanocomposite films prepared by the CE method, the mechanical strength and elongation were significantly increased by up to about 40% compared with the pure chitosan films. On the other hand, the ordered and porous multilayered pure chitosan films prepared by the SAC method showed significantly lower tensile strength and elongation compared to the pure solid chitosan films. However, the relative enhancement of the mechanical properties of multilayered MWCNT/chitosan nanocomposites with porosity was higher, especially in terms of the elongation, which showed a twofold improvement in strain. The relaxed bond, which could be a relatively strong hydrogen bond, between the functional groups in the chitosan chains and the functionalized surface of the MWCNTs might be stretched under stress, thereby improving the ductility of the multilayered nanocomposite films. In addition, the viscoplastic behavior of the films by the CE method could become more active with increasing strain rate. Interestingly, ordered and porous pure chitosan films did not reveal the viscoplastic behavior; it rather presented strain softening and viscoelastic characteristics. However, the interaction between the chitosan chains and the surface-modified MWCNTs could regenerate viscoplasticity of the chitosan films.

1. Introduction

Recently, polymeric materials have been studied widely for biological applications [1,2], especially for use in electrochemical sensing, biosensors [3], flow sensing [4], biofuel cells based on direct electrotransfer [5,6], drug delivery, and tissue engineering [7,8]. However, the rather poor mechanical, electrical, and thermal properties of polymeric materials limit their use. In particular, good mechanical properties are of fundamental importance in the fabrication of robust polymeric devices. Polymer-based nanocomposites have been developed over the past few decades to overcome this innate mechanical limit of polymers. The nanocomposites consist of nanostructured filler materials, i.e., clay platelets [9,10], inorganic nanoparticles [11,12], and carbon nanotubes (CNTs) [13,14]. Among these filler materials, CNTs are the most attractive due to their excellent properties [15,16]. It is well known that CNTs possess extraordinarily high aspect ratios, thermal and electro-activities [17], unique atomic structures [18,19], and remarkably good mechanical properties [14,13]; these properties suggest that they can be used for preparing reinforced polymer composites. However, the agglomeration of CNTs limits their application because this behavior could lead to many nanoscale and/or microscale defects, which would diminish the mechanical performance and physical properties of the composites. There are some useful and effective ways of preparing well-dispersed CNTs: (1) attaching a functional group on the surface of the CNT, which is the most ideal and practical method, (2) using ultrasonication for dispersing CNTs, and (3) using a surfactant for a well-dispersed CNT solution [18]. With these methods, reactive functional groups can be formed on the surface of the CNTs. These functional groups greatly promote the binding of the CNTs with a variety of polymeric matrices [14]. Facilitating the dissolution of CNTs in chitosan solution in this way could

* Corresponding authors. Tel.: +82 55 350 5301; fax: +82 55 350 5279.
E-mail addresses: jaebeom@pusan.ac.kr (J. Lee), dlee@pusan.ac.kr (D. Lee).
[1] Equally contributed.

0921-5093/$ – see front matter © 2011 Elsevier B.V. All rights reserved.
doi:10.1016/j.msea.2011.05.028

improve the mechanical properties of the nanocomposite. Moreover, because of the presence of amino groups in the chitosan, hydrogen bonding between the functionalized CNT and the chitosan is potentially achievable. Hydrogen bonding is expected to enhance the solubilization of the CNT in chitosan and improve the interfacial strength as well as the mechanical performance of the nanocomposite [20]. Many research groups have investigated the mechanical properties of polymer-CNT composites, especially the chitosan/CNT composite because of its potential applications [14,21,22]. With the incorporation of only small amount of MWCNTs (~1 wt%) into the chitosan matrix, the tensile modulus and strength of the nanocomposites were improved greatly by about a factor of two.

From this literature survey, there has been a lack of research on the detailed area of the nanoscale interfaces between the composite materials, which is where the physical and mechanical properties of the composites are determined. Nanoscopic observation via nano-indentation can reinforce the comprehensibility of macroscopic investigation in the prepared nanocomposites. Among many kinds of polymers (for instance, hydrogel [8], epoxy [18], and chitosan [12,1,23]) widely used as matrices for fabricating biologically accessible nanocomposites, chitosan, a well-known and plentiful natural hydrophilic biopolymer [24], has been widely used in various research fields such as water treatment, separation membranes, food packaging, tissue engineering, and drug delivery [14]. Therefore, it is believed that well-combined nanocomposites of CNTs and chitosan could find many potential applications, particularly in biomechanical engineering.

In this study, we used two methods for the preparation of nanocomposite films: (1) a simple and fast sublimation-assisted compression (SAC) method to construct uniformly structured films, using inherited polymeric phase separation during the solidification process [12], which provides a novel polymer-inorganic microstructure. The most remarkable advantage of this method is that the inner structure of the composite in its solution state can be retained, (2) a casting-evaporation (CE) method, in which a chitosan/MWCNT composite with compact structure and flexible properties is fabricated. With the two ways to manufacture the nanocomposite films, we discuss how the CNTs behave in the unique structures of the chitosan matrix, and how this behavior enhances the mechanical properties of the nanocomposites.

2. Experimental procedures

2.1. Materials

MWCNT was purchased from the company CNT Co. Ltd., (Incheon, Korea). The MWCNTs with 10–40 nm in outer diameter, 1–25 μm in length and >93% purity were produced by thermal chemical vapor deposition method. Chitosan with deacetylation >75% and viscosity of 800.00 cps was obtained from Aldrich. Acetic acid with purity of >97% was used in our experiment without further purification.

2.2. Acid treatment of MWCNTs

The raw MWCNT powder, as we know, is non-dispersed in water. Here, we suggest an optimized step for the surface modification of the MWCNTs by heating at reflux in 61.5% nitric acid with magnetic stirring for 2 h. In our experiment, the disassembly of the MWCNT aggregates was induced through the introduction of ethanol, with continuous sonication to shorten the MWCNTs. Using this procedure, most MWCNT chunks were disassembled to smaller sizes (sub-micrometer scale). However, the treatment was insufficient for the formation of a stable colloidal suspension in the aqueous state, so acidic treatment was carried out to introduce hydrophilic groups, i.e., the carboxyl groups introduced partly on the sidewalls of the CNTs as well as at the ends. In the acidic treatment, 15.5 mg of MWCNT was dispersed in 35 mL concentrated nitric acid, and the solution was boiled under reflux conditions for 2 h. Then the specimen was diluted, separated, filtered and subsequently washed with distilled water until a neutral solution was obtained. The acid-treated MWCNTs with diameter of 10–20 nm and length of 200nm–5 μm were stable for more than one month, without signs of aggregation.

2.3. Fabrication of chitosan/MWCNT nanocomposite solution

The acid-treated MWCNTs (15.5 mg) were dispersed in 200 mL distilled water, and ultrasonication (8510E-DTH, Bransonic, USA) was performed for at least 30 min to make sure that the MWCNTs were dispersed homogenously. A 1.0 wt% chitosan aqueous solution was prepared by dissolving the chitosan powder (0.5 g) in 0.1 M acetic acid. The mixture was stirred at room temperature for 2 h to obtain a homogeneous polymer solution. 20 mL of the prepared MWCNT solution was then added to the chitosan solution to give the chitosan/MWCNT nanocomposite solution, which was stirred for 2 h. Then the solution was agitated vigorously in an ultrasonic bath for approximately 1 h until the MWCNTs showed no sign of precipitation or aggregation. Before ice-molding, the zeta potential (ZS-nano, Malvern, UK) of the aqueous acetic acid solution of chitosan/MWCNT was measured in order to determine the dispersity of the colloids.

As stated in Section 1, two methods were adopted for the fabrication of the chitosan/MWCNT nanocomposite films in this study. The detailed methodologies are explained below.

2.3.1. Freeze-drying associated with the sublimation and compression (SAC) method

First, chitosan/MWCNT nanocomposite films were prepared by a freeze-drying process associated with the SAC method. In this procedure, the foam was created by solid–liquid phase separation from the mixture, and the acetic acid solvent was subsequently removed by sublimation at ultra-low temperature. In a typical experiment, 10 mL of chitosan/MWCNT mixture was cast into a Petri dish, and rapidly transferred to a deep freezer (NIHON FREEZER, NF-75SF, Japan) at −78 °C for 4 h; thus, the mixture was solidified, and solid–liquid phase separation was induced. The frozen mixture was then immediately transferred to a freeze-dryer (FreeZone, Labconco Co., USA) at −86 °C and 0.120 mbar for 42 h to remove solvents from the frozen structure. The foam-type nanocomposite was then pressed at room temperature into a flexible thin film at a load of 10 tons for 10 s using a vertical presser (Hyundai Mechanics Inc., Korea).

2.3.2. Casting-evaporation (CE) method

After the preparation of the chitosan/MWCNT solution, the mixture was left to stand for 1 h until the air bubbles disappeared. Then, vigorous sonication was performed for 30 min to degas the solution, and to ensure that a homogenous solution was obtained, with well-dispersed MWCNTs. In a typical casting-evaporation process, 10 mL of the prepared chitosan/MWCNT solution was cast into a dry aluminum Petri dish in a dust-free desiccator, and allowed to dry in air at 25 °C for 24 h until the film peeled out naturally. The obtained chitosan/CNT film was kept in a desiccator.

2.4. Tensile and nanoindentation tests

The mechanical properties of the nanocomposite films were investigated using a tensile test system (LRX*Plus*, Lloyd Instruments, UK) and a nanoindentation system (Nanoindenter™,

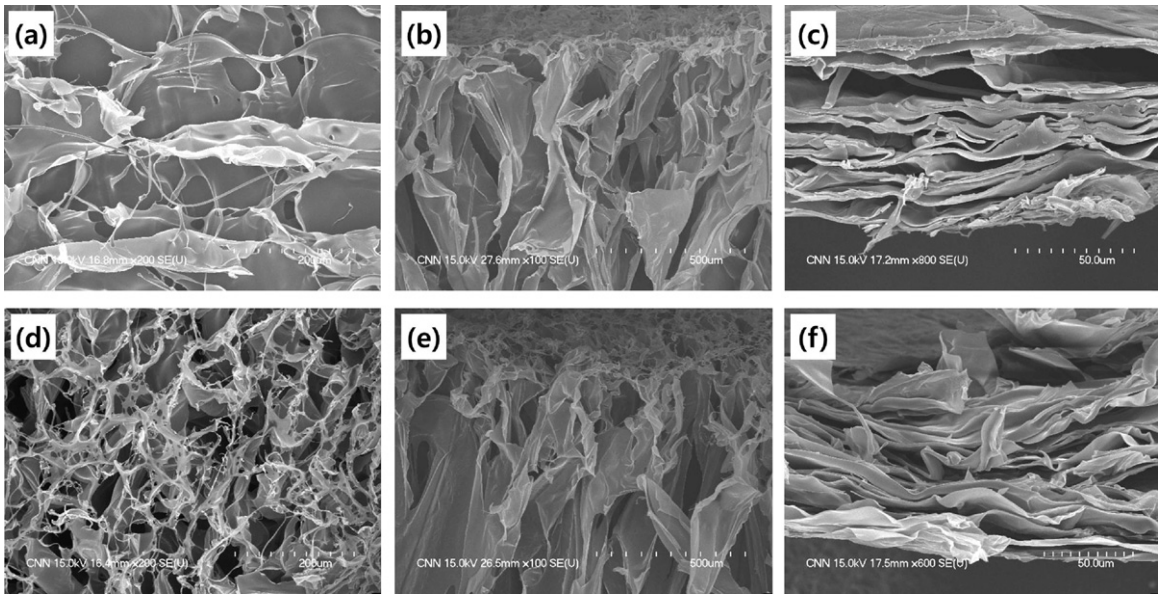

Fig. 1. SEM micrographs of pure chitosan (a)–(c) and chitosan/MWCNT nanocomposite (d)–(f), films fabricated by the freeze-drying method at −78 °C. The surface and cross-section images of the films before pressing are presented in (a) and (d), and (b) and (e), respectively. Figures (c) and (f) show the films after pressing.

Agilent Tech., USA). Specimens for the tensile test (gauge section: 5.0 mm × 8.0 mm, 75 μm thickness) were cut from the chitosan films with or without MWCNTs. The tensile tests were conducted in air using a 1-kN load cell at a crosshead speed of 10 mm/min. The results presented here are the average values obtained from at least three specimens. To prevent the thin specimens slipping from the grip, thin glass was attached to the grip part of the tester with superglue. We presumed that the thin glass on the grip did not affect the mechanical properties of the specimens, because the specimens fractured within the gauge length.

For the nanoindentation experiments, the films were glued onto an aluminum holder. The experiments were conducted with a Nanoindenter XP™ under strain rate control to no more than ~20% of the composite film thickness. At a given force level, the data were averaged from at least 15 indentations, with scatter indicated by standard deviation in displacement. A three-sided pyramid (Berkovich) diamond tip was used for this study. An indentation strain rate of either 0.01 or 0.05 s^{-1} was adopted for a predetermined load, followed by a constant load dwell for either 10 or 20 s. A constant indentation strain rate, $(dh/dt)/h$, was obtained with constant $(dP/dt)/P$ (in which h = displacement, t = time, P = load) tests [25], which allowed us to evaluate the hardness of the materials independently of the indentation depth [26]. Unloading was achieved under strain rate control, using the same rate as for the indentation. The elastic stiffness modulus E was determined from the unloading slope. The continuous stiffness measurement technique [25] allows the unloading slope to be determined as a function of depth by superimposing a dither on the displacement. The hardness H of the film was determined as the ratio of the indentation force to the projected area of contact on the original surface [25].

3. Results and discussion

3.1. Microstructures

Fig. 1 shows the SEM micrographs of the chitosan films fabricated by the SAC method, with the presence or absence of MWCNTs, at −78 °C. Fig. 1((a, top view) and (b, side view)) and ((d, top view) and (e, side view)) present the microstructures of the chitosan foams before compression, without and with MWCNTs, respectively. In addition, Fig. 1(c) and (f) are representative SEM images of the films after compression, without and with MWCNT reinforcement, respectively. As shown in Fig. 1, foam structures were formed due to the sublimation of the solvent, and well-dispered MWCNTs are easily recognized around the pore walls, particularly in Fig. 1(d). The porous structures of the films containing MWCNTs are relatively more regular compared to those of the films without CNTs, probably as a result of the structures being more layered (compare Fig. 1(c) and (f)). Presumably, during the 42 h of lyophilization to remove the solvents from the frozen structure of the well-dispersed polymer-MWCNT composites, MWCNT could block the blasting of polymeric chains that is caused by sublimation of the solvent.

3.2. Tensile test

The tensile test results are shown in Fig. 2 as typical stress–strain curves of the chitosan films fabricated by the two different methods. Curves A and B were obtained for films fabricated by the CE method, and curves C and D for those created by the SAC method. Curves B and D are the results for the films reinforced with MWCNTs. Average values for the Young's modulus, yield, and tensile strength of the films are listed in Table 1. Because no distinct yield point was observed, we used a 0.2% offset concept to measure

Table 1
Mechanical properties under tension of the pure and nanocomposite chitosan films fabricated by the two methods.

	EC		SAC	
	Chitosan; A	Chitosan + CNT; B	Chitosan; C	Chitosan + CNT; D
Modulus (MPa)	1288	1613	484	502
UTS (MPa)	70.19	99.22	14.77	20.58
Elongation (%)	8.86	12.36	4.43	9.82

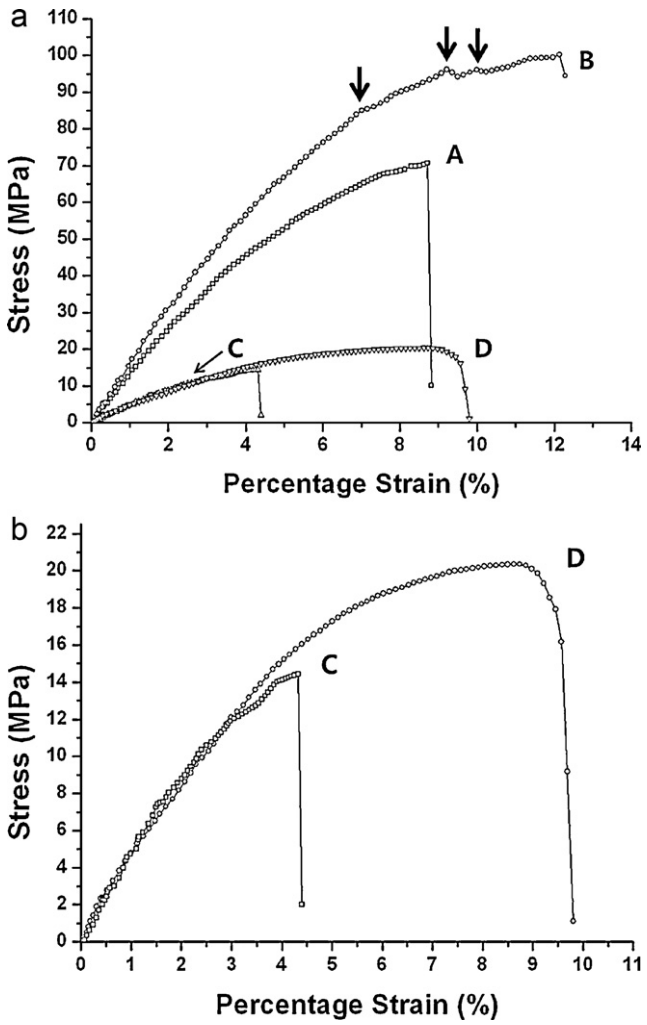

Fig. 2. (a) Stress–strain curves of chitosan/MWCNT nanocomposite films prepared by the CE method (A and B) and the SAC method (C and D). (b) Rescaled curves C and D.

the engineering yield strength. Fig. 2 does not show the averaged curves, but rather gives a representative curve similar to the averaged values of each test condition, because this better reflects the detailed deformation behavior of the films.

As seen in Fig. 2(a), adding MWCNTs to chitosan films prepared by the CE method clearly increases the strength and elongation by up to about 40%. The SEM images of the fracture surfaces of the specimens (shown in Fig. 3(a)) indicate a cleavage fracture facet along the crack-opening direction. The cracks indicated by the arrows in Fig. 3(a) were presumably caused by crazing, which is one of the main fracture mechanisms of polymeric materials. Although crazing involves some localized plastic deformation, the critical stress thickens the crazes through the growth of fibrils that nucleate cracks. In Fig. 3(a), the fibrils can be recognized inside the crack opening indicated by the white arrows; the growth of these fibrils causes the nucleation of a crack, and the material will fail when the fibril reaches a critical length [27].

Significant improvements in tensile strength and elongation were observed when MWCNTs were added to chitosan films. As shown in Fig. 2(a), the tensile strength and elongation were enhanced by 40% and 43%, respectively, by the addition of MWCNTs. Interestingly, the number of cracks caused by crazing decreased dramatically with the addition of MWCNTs, as shown in Fig. 3(b). In addition, stepped-fracture surfaces as well as dithering were observed, as indicated by the arrows in Fig. 3(b) and graph B in Fig. 2(a), respectively. Presumably, the dithering in the stress–strain curve B is correlated with the stepped-fracture surface, suggesting that cracks caused by crazing may be suppressed by the addition of MWCNTs.

Table 2
Elastic modulus and hardness of pure and nanocomposite chitosan, determined by nanoindentation tests.

	EC		SAC	
	Chitosan	Chitosan + CNT	Chitosan	Chitosan + CNT
E (MPa)	3839	5039	436	566
H (MPa)	127	185	19	26

Curves C and D in Fig. 2(a) are rescaled in Fig. 2(b) to show the graph in detail. We see that multilayered chitosan films fabricated through the SAC method show significantly lower mechanical properties than the films obtained by the CE method. Even though the films are layered structures, they could be intrinsically brittle because they were created from a medium that was originally porous. However, MWCNT-reinforced nanocomposite films exhibit a much higher tensile strength (an increase of about 40%), and a two-fold improvement in elongation (about 120% increase). Fig. 4 shows the fracture surface of pure chitosan and chitosan/MWCNT nanocomposite films fabricated at −78 °C by the SAC method. Fig. 4(a) and (b) are representative fracture surfaces of the pure chitosan multilayered chitosan film. This shows an irregular feature: there is no shear band or crazing on the fracture surfaces, but sudden failure is observed after reaching ultimate tensile strength. Note that Fig. 4(b) is an enlarged micrograph of the circle in Fig. 4(a). Fig. 4(c) and (d) present the fracture surfaces of the multilayered chitosan/MWCNT nanocomposite films. Although some of the reinforcing MWCNTs were pulled out, a 120% increase in elongation was observed. Therefore, we suggest that the interaction between the MWCNTs and the foamed chitosan chains probably renders the porous medium less brittle. The acid-treated MWCNTs contain many defects and hydrophilic groups such as diphenol, –OH, and –COOH, which might help the interaction between the MWCNTs and chitosan foam chains, thus improving the ductility of the multilayered nanocomposite films [14]. A strong hydrogen bond between the functional groups of the chitosan and the functionalized surface of the MWCNTs might enhance the interfacial adhesion that noticeably reduces the brittleness of the porous materials [14].

3.3. Nanoindentation test

Nanoindentation tests were employed to understand the hardness and elastic modulus of the films, as well as the strain-rate sensitivity of the materials. Table 2 lists the values of elastic modulus (Young's modulus), *E* and hardness, *H*, for various specimens with MWCNTs, obtained at an indentation depth of less than 20% of the film thickness to minimize substrate effects. As shown in Table 2, MWCNT-reinforced nanocomposites obtained through both the EC and SAC methods show increases in Young's modulus and hardness of up to about 46%. This is consistent with the results of the tensile tests. Curiously, we observed that in the case of the specimen prepared by the EC method, the Young's modulus obtained from the nanoindentation test was significantly higher than that from the tensile test. Similar values obtained from nanoindentation were reported by Fan et al. [17], both in pure chitosan and in nanocomposite chitosan with graphene as the reinforcing material. This could be explained by considering two main issues: (1) the substrate effect, which is commonly observed in the indentation test; and (2) the fact that the modulus from the nanoindentation test based upon the Oliver–Pharr method [25] might not be perfectly suitable for viscoplastic materials [28]. Work is underway on

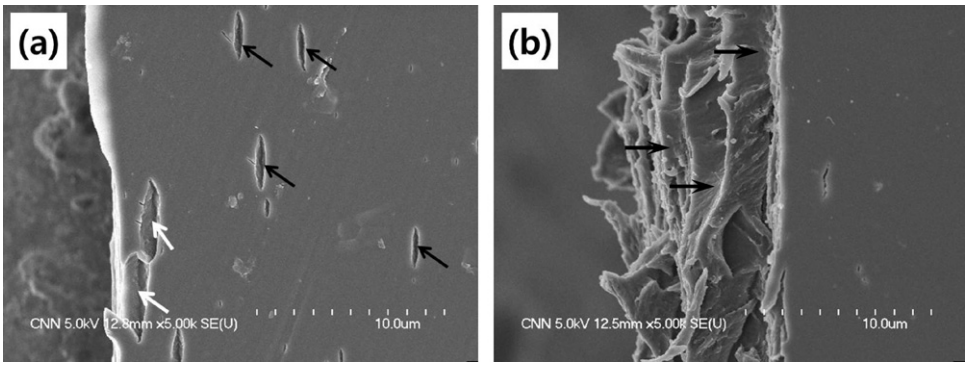

Fig. 3. Fracture surface of pure chitosan and chitosan/MWCNT nanocomposite films fabricated by the CE method: (a) cracks formed by crazing on pure chitosan films and (b) stepped-fracture surfaces of chitosan/MWCNT composite film.

a new experimental approach that should avoid such measurement errors.

In addition, time-dependent deformation was evident for the larger displacements at the holding segment with longer dwell times. This result is not presented in this paper, but a displacement about 2.2 times larger was observed at the maximum load for all specimen conditions (e.g., for chitosan/MWCNT prepared by the EC method, ~306 nm and ~139 nm displacement when holding for 20 s and 10 s, respectively).

Load–displacement curves of the nanoindentation experiments for the multilayered pure chitosan and the chitosan/MWCNT nanocomposite are shown in Fig. 5. Curves A and B show the load–displacement curves of the multilayered pure chitosan films, and C and D show those for the chitosan/MWCNT nanocomposite films. Note that we used average load–displacement data to plot the curves. As mentioned in Section 2, we varied the strain rate, using values of 0.01 s^{-1} (curves A and C) and 0.05 s^{-1} (curves B and D). The slopes indicated in the graphs of the loading curves C and D in Fig. 5 increase with strain rate, indicating a strain-rate dependence of constitutive relations, i.e., an increase of the resistance of the materials to indentation with strain rate. We, therefore, presume that the films exhibit viscoplastic behavior (as is commonly seen in polymers), and/or viscoelastic behavior (time-delayed reversible strain). As already observed in the tensile test, the observation of significant permanent plastic deformation suggests that the material is somewhat viscoplastic. In polymers, the rate dependence of plastic deformation and creep (i.e., viscoplastic properties) is a commonly observed phenomenon. However, it is worth mentioning that, interestingly, multilayered pure chitosan films show the opposite results: a higher strain rate gives rise to a lower sustainable load at a given displacement (curves A and B). Well-dispersed MWCNTs around the pores meant that a uniform distribution of MWCNT was achieved between layers after pressing, as observed in the cross-sectional images in Fig. 1 and fracture surfaces in Fig. 4. The well-distributed MWCNTs might block the easy collapse of the porous medium. On the other hand, the walls of pore cells in porous

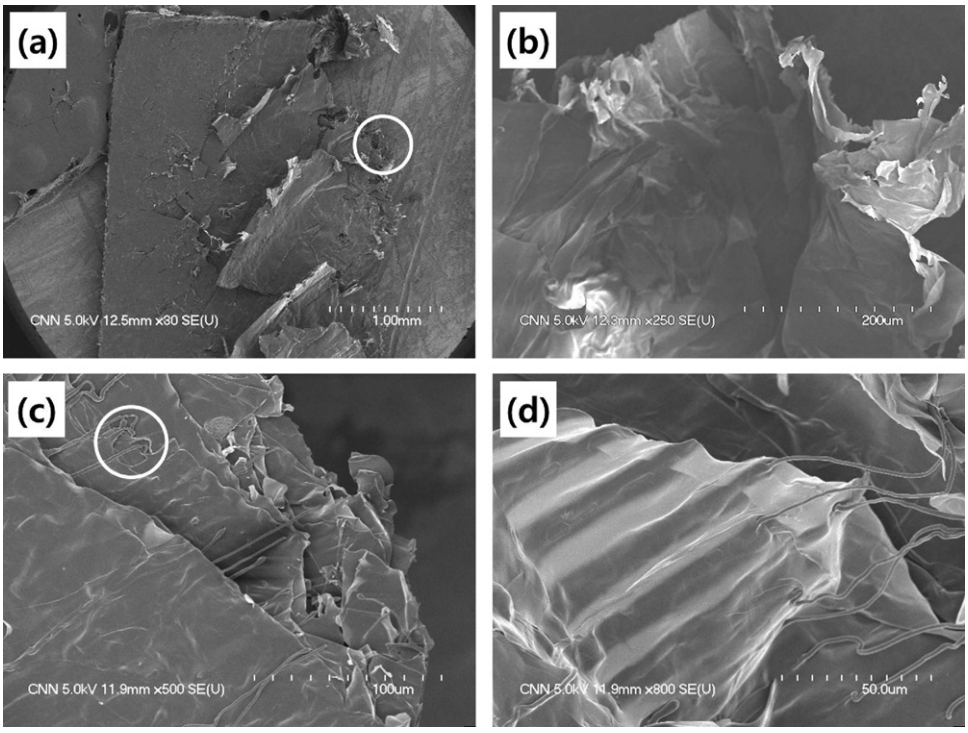

Fig. 4. Fracture surface of pure chitosan and chitosan/MWCNT nanocomposite films fabricated at −78 °C by freeze-drying associated with the SAC method: (a) and (b) irregular fracture surface of pure chitosan films; (b) enlarged micrograph of the circle in (a); (b) and (c) fracture surfaces of chitosan/MWCNT composite films; (d) enlarged micrograph of the circle in (c).

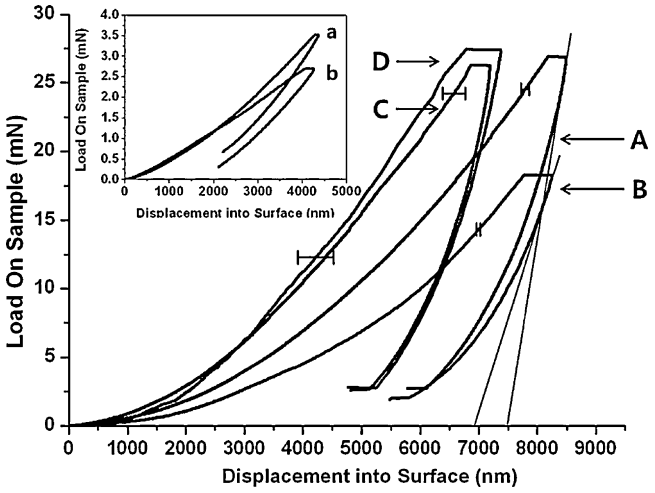

Fig. 5. Load–displacement curves of the films fabricated by the SAC method without MWCNT (A and B, a and b) and with MWCNT (C and D). A and C are the load–displacement curves for 0.01 s^{-1}, and B and D are those for 0.05 s^{-1}. The inset shows the load–displacement curves for the low-load experiment.

media might collapse readily under fast loading conditions, and because there is no resisting medium to hold the load, a higher and faster loading rate causes the cells to collapse more easily. In addition, we observe that the slope of the unloading curve B is slightly lower than that of curve A, which indicates that a higher strain rate corresponds to more recovery, as the unloading curves represent the elastic recovery of the materials. We speculate that the viscoelastic behavior of the multilayered and foamed pure chitosan could become more pronounced with increasing strain rate. On the other hand, the interaction between the chitosan polymeric chains and the surface-modified MWCNTs could dampen the viscoelastic characteristics. Further research, including computational simulation, is currently being undertaken to gain a fuller understanding of the interactions between the chitosan molecules and CNTs, as well as the interaction of molecules in the multilayered and foamed pure chitosan.

4. Conclusion

A multi-performance chitosan nanocomposite reinforced with surface-modified multiwalled carbon nanotubes (MWCNTs) was fabricated through two methods: a freeze-drying-assisted sublimation and compression (SAC) method and a casting-evaporation (CE) method. The morphology and mechanical properties of the chitosan with or without MWCNT films were investigated by scanning electron microscopy and microtensile/nanoindentation systems, respectively. Strain rate sensitivity was also investigated by nanoindentation test. Dense and translucent solid chitosan films were obtained by the CE method whereas one could attain a unique ordered and porous multilayers chitosan films by the SAC method. Crazing phenomenon was observed in the pure solid chitosan but it almost diminished by addition of MWCNTs, which resulted the improvement of the mechanical properties of the nanocomposite films. On the other hand, bonding strength between chitosan layers could be one of the main factors to determine the mechanical properties of the films by the SAC method. Comparing to the solid chitosan films, mechanical properties, especially tensile stress and ductility, were notably lower in multilayered chitosan films, which could be owing to porosity. However, well-dispersed MWCNTs in ordered and porous multilayered chitosan films by the SAC method significantly improved the ductility of the chitosan films (more than 100%). Presumably, bonding between the functional groups in the chitosan chains and the functionalized surface of the MWCNTs are weak but stretchable bonding named as 'relaxed bonding', a relatively strong hydrogen bond. In addition, the viscoplastic behavior of the films by the EC method could become more active with increasing strain rate. Interestingly, ordered and porous pure chitosan films did not reveal the viscoplastic behavior; it rather presented strain softening and viscoelastic characteristics. However, the interaction between the chitosan chains and the surface-modified MWCNTs could regenerate viscoplasticity of the chitosan films.

Further research, including computational simulation, is being undertaken in order to understand the interactions between the chitosan molecules and CNTs, as well as the interactions among molecules in the multilayered pure and nanocomposite chitosan films. All the assessments showed that flexible MWCNT/chitosan composite films with multilayered porous morphologies have great potential for applications in biomedical engineering.

Acknowledgements

This work was supported by the New & Renewable Energy Program of the Korea Institute of Energy Technology Evaluation and Planning (KETEP) grant (No. 20103020010050) funded by the Ministry of Knowledge Economy, Republic of Korea (J.L.). This research was also supported by Basic Science Research Program through the National Research Foundation of Korea (NRF) funded by the Ministry of Education, Science and Technology (2010-0025175), and partially supported by the 2010 Specialization Project Research Grant funded by the Pusan National University (D.L.).

References

[1] F. Chen, Z.C. Wang, C.J. Lin, Mater. Lett. 57 (2002) 858.
[2] Y. Zhang, M. Ni, M. Zhang, B. Ratner, Tissue Eng. 9 (2003) 337.
[3] X.L. Luo, J.J. Xu, J.L. Wang, H.Y. Chen, Chem. Commun. 2005 (2005) 2169.
[4] S. Ghosh, A.K. Sood, N. Kumar, Science 299 (2003) 1042.
[5] M. Zhang, A. Smith, W. Gorski, Anal. Chem. 76 (2004) 5045.
[6] Y. Liu, L. Liu, S. Dong, Electroanalysis 19 (2007) 55.
[7] B.S. Harrison, A. Atala, Biomaterials 28 (2007) 344.
[8] F. Xie, P. Weiss, O. Chauvet, J. Le Bideau, J.F. Tassin, Mater. Sci.-Mater. Med. 21 (2010) 1163.
[9] C. Tang, L. Xiang, J. Su, K. Wang, C. Yang, Q. Zhang, Q. Fu, J. Phys. Chem. B 112 (2008) 3876.
[10] M.J. Solomon, A.S. Almusallam, K.F. Seefeldt, A. Somwangthanaroj, P. Varadan, Macromolecules 34 (2001) 1864.
[11] Y. Zhang, J.R. Venugopal, A. El-Turki, S. Ramakrishna, B. Su, C.T. Lim, Biomaterials 29 (2008) 4314.
[12] F. Sun, B.K. Lim, S.C. Ryu, D. Lee, J. Lee, Mater. Sci. Eng. C 30 (2010) 789.
[13] C. Lau, M.J. Cooney, P. Atanassov, Langmuir 24 (2008) 7004.
[14] S.F. Wang, L. Shen, Y.J. Tong, Biomacromolecules 6 (2005) 3067.
[15] A.K. Kota, B.H. Cipriano, D. Powell, S.R. Raghavan, H.A. Bruck, Nanotechnology 18 (2007) 505705.
[16] A.K. Kota, B.H. Cipriano, M.K. Duesterberg, A.L. Gershon, D. Powell, S.R. Raghavan, H.A. Bruck, Macromolecules 40 (2007) 7400.
[17] H. Fan, L. Wang, K. Zhao, N. Li, Z. Shi, Z. Ge, Z. Jin, Biomacromolecules 11 (2010) 2345.
[18] X. Gong, J. Liu, S. Baskaran, R.D. Voise, J.S. Young, Chem. Mater. 12 (2000) 1049.
[19] Z.L. Wang, P. Poncharal, W.A. De Heer, Pure Appl. Chem. 72 (2000) 209.
[20] W. Tang, M.H. Santare, S.G. Advani, Carbon 41 (2003) 2779.
[21] G.M. Spinks, S.R. Shin, G.G. Wallace, P.G. Whitten, S.I. Kim, S.J. Kim, Sens. Actuators B: Chem. 115 (2006) 678.
[22] L. Liu, A.H. Barber, S. Nuriel, H.D. Wagner, Adv. Funct. Mater. 15 (2005) 975.
[23] S.H. Kim, B.K. Lim, F. Sun, K. Koh, S.C. Ryu, H.S. Kim, J. Lee, Polym. Bull. 62 (2009) 111.
[24] de Fatima Ferreira Soares N, John Wiley & Sons, Inc. (2008) 107.
[25] W.C. Oliver, G.M. Pharr, J. Mater. Res. 7 (1992) 1564.
[26] B.N. Lucas, W.C. Oliver, Metall. Mater. Trans. A 30 (1999) 601.
[27] N. Saad-Gouider, R. Estevez, C. Olagnon, R. Seguela, Eng. Fract. Mech. 73 (2006) 2503.
[28] H. Lu, B. Wang, J. Ma, G. Huang, H. Viswanathan, Mech. Time-Depend. Mater. 7 (2003) 189.